Combined Structural and Dimensional Synthesis of a Parallel Robot for Cryogenic Handling Tasks

6

Moritz Schappler, Philipp Jahn, Annika Raatz and Tobias Ortmaier

Abstract

The combined structural and dimensional synthesis is a tool for finding the robot structure that is suited best for a given task by means of global optimization. The handling task in cryogenic environments gives strong constraints on the robot synthesis, which are translated by an engineering design step into the combined synthesis algorithm. This allows to reduce the effort of the combined synthesis, which provides concepts for alternative robot designs and indications on how to modify the existing design prototype, a linear Delta robot with flexure hinges. Promising design candidates are the 3PRRU and 3PRUR, which outperform the linear Delta (3PUU) regarding necessary actuator force.

Key words:

Combined structural and dimensional synthesis • Cryogenic work environment • Flexure hinge • Joint range constraint • Parallel robot

M. Schappler (✉) · T. Ortmaier
Leibniz Universität Hannover, Hannover, Germany
E-mail: moritz.schappler@imes.uni-hannover.de

Institut für Mechatronische Systeme, An der Universität 1, 30823 Garbsen, Germany

P. Jahn · A. Raatz
Institut für Montagetechnik, An der Universität 2, 30823 Garbsen, Germany

T. Schüppstuhl et al. (eds.), *Annals of Scientific Society for Assembly, Handling and Industrial Robotics 2021*,
https://doi.org/10.1007/978-3-030-74032-0_6

1 Introduction and State of the Art

The automation of handling processes is an omnipresent factor in industry and research institutions. A robot-supported automation solution is also desirable for extremely niche areas such as the cryogenic storage of biological materials [1]. The development of task-adapted structures for such exceptional cases poses significant challenges for designers: From an almost infinite variety of design possibilities, the optimal design for the task and the underlying geometric and situational constraints must be found. Even if the application's basic parameters are entirely known, it is impossible to manually design and evaluate all possible variations of the robot structure. One approach to realize all these variations is the computer-aided structural analysis using optimization algorithms. In this paper's context, such an optimization strategy is investigated using the example of a parallel robot for use in a cryogenic working environment, and the results are compared with the structure aimed at so far.

It is well established that the performance of parallel robots is highly subject to their kinematic parameters which can be determined for a given structure in a *dimensional synthesis* [2]. The selection of the specific structure, i.e. the *structural synthesis*, is usually performed manually with the help of design and construction principles [3]. As the systematic structural synthesis of parallel robots by means of screw theory [4] or evolutionary morphology [5] provides a high number of suitable structures, the selection of the optimal solution is an exhaustive task. The concept of *combined structural and dimensional synthesis*, introduced in [6] for parallel robots, assumes that the optimal solution can be found by independently optimizing all possible structures and selecting the best one. This requires a high number of simulations of the robots kinematics and dynamics and is only applicable with a general, yet efficient model and its implementation and a suitable optimization algorithm.

The engineering solution to the considered handling problem is the linear Delta robot. It was already subject to parameter optimizations regarding workspace-related objectives [7] or objectives related to kinematics and dynamics [8]. A dimensional synthesis for both the classical Delta robot and the linear Delta was performed in [6] and used for a systematic comparison of the two.

The comparison of multiple parallel robots (whether two different structures or two sets of parameters for one structure) has to be performed using multiple criteria [2], representing all requirements to the robot. Often genetic algorithms are employed such as the Strength Pareto Evolutionary Algorithm [6, 8] or Nondominated Sorting Genetic Algorithm [9]. Particle swarm optimization (PSO) is reported to have better convergence than genetic algorithms for constraint nonlinear optimization problems. One reason is that not only the parameters of the current iteration carry information but also past iterations are taken into account to generate a new set of parameters [10]. Constraint handling [11] is central for the validity of the robot synthesis and the convergence of the PSO.

This paper presents results for the combination of the engineering solution and the combined synthesis presented above by taking the most restricting constraints of the task into

account for the structural synthesis and thereby vastly reducing the amount of possible structures, for which a dimensional synthesis has to be performed. The contributions of the paper are

- transferring the specific constraints of cryogenic handling tasks in a suitable form for parameter optimization,
- proving the applicability of multi-objective PSO on the dimensional synthesis of parallel robots as opposed to genetic algorithms in literature,
- presenting design alternatives of the linear Delta for cryogenic handling.

The remainder of the paper is structured as follows: Sect. 2 gives an overview of the constraints of the cryogenic handling task. The engineering approach to the robot synthesis is presented in Sect. 3, followed by the combined synthesis in Sect. 4. The results are discussed in Sect. 5.

2 Task Definition and Requirements

The freezing and storage of biological material in biobanks at temperatures below −130 °C is commonly referred to as cryopreservation. Manual handling of biological or toxic samples is still the norm in research institutions. In such systems, the samples are often transferred in, out, or moved by hand using bulky protective clothing. This poses considerable risk of injury to the worker through cold burns as well as a threat to the sample integrity.

To overcome these problems, a parallel robot for the realization of full automation is being developed.

2.1 Requirements for the Parallel Robot

The possibility of placing the drives in the warm area outside the storage container makes the parallel structure interesting for use in cryogenic environments, as it allows the drive technology to be decoupled from the cryogenic handling area. The drive movement is then transferred to the end effector platform via passive joints.

The robot to be developed is subject to a number of geometric constraints. The installation space dimensions correspond to the internal dimensions of the Cryotherm BIOSAFE cryogenic storage container, which is to be used for the demonstrator (Fig. 1, left). The usable interior space (height 680 mm and inner diameter 600 mm) is highlighted by the red dashed line in the middle of Fig. 1.

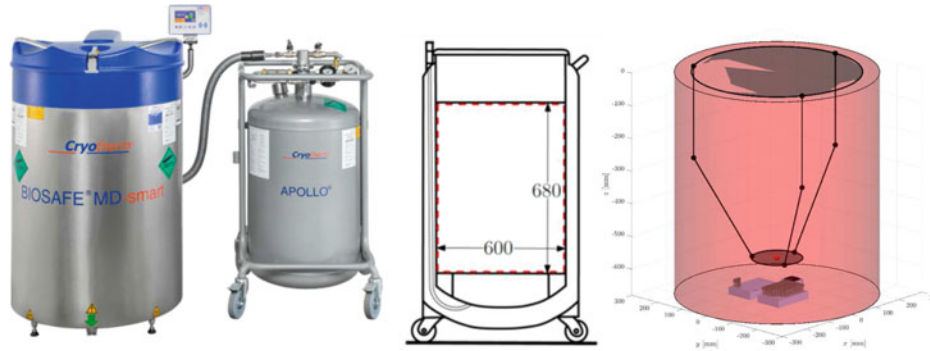

Abb. 1 Left: Cryotherm BIOSAFE cryogenic storage container, middle: dimensions of the installation space, right: robot handling scenario in a MATLAB simulation

For the storage of sample tubes in the cryogenic storage container, racks of type Micronic 96-3 are to be used, between which the tubes are to be transferred by the manipulator (see Fig. 1, right). The rack's height, including the sample tubes, is 45.2 mm, and the sample tubes height is 44 mm. To avoid collisions between the sample tubes to be transferred and the sample tubes stored in the racks during the pick-and-place process, the height of the necessary working space is set to 110 mm, to ensure a safety distance of approx. 20 mm. To keep the working space area as small as possible, the racks are placed lengthwise next to each other. The space next to it is used for a scanner, which will be used to identify the sample tubes. The resulting square area of the working space is 200 mm wide. To ensure a good thermal insulation of the cold area, the moving parts of the parallel robot have to cover a constant area on the cap of the container, favoring a vertical arrangement of linear drives.

2.2 Requirements for the Solid-State Joints

Extremely high demands are placed on the robot's passive joints: The extreme temperatures of below −130 °C do not allow the use of classic rigid body systems such as ball joints due to freezing of lubricants or jamming of components through cold shrinking. To avoid these disadvantages, flexure hinges in the form of cohesive swivel joints are used. Due to their monolithic structure, there are no parts that move against each other. Clamping is not possible and, in addition, the use of lubricants is not necessary. A major disadvantage of flexure hinges, however, is their low range of angles compared to conventional joints. Therefore, a parallel robot based on flexure hinges – depending on the required rotation angle limitation – can have a significantly reduced workspace compared to an otherwise identical parallel robot with conventional joints [12]. Furthermore, the negative influence of

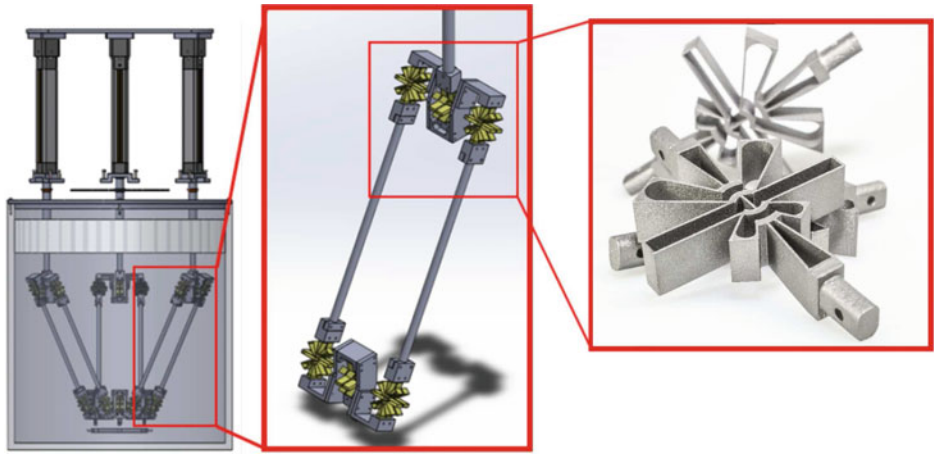

Abb. 2 Left: CAD rendering of a possible parallel robot structure (from [15]), middle: detail on the leg chain, right: flexure hinge photograph

cryogenic environmental conditions on flexure hinges' deformation behavior has not been investigated in detail so far.

A cascading flexure hinge, depicted in the right of Fig. 2, was developed based on the work of Fowler and Henein [13, 14]. The cohesive hinge is made of the titanium alloy TiAl6V4 by laser sintering due to this material's superior properties under cryogenic conditions. In preliminary work [15], it could be shown that a rotation angle of up to 30° (in one direction from the neutral position) and therefore a joint range of up to 60° can be realized with the developed flexure hinges. This *joint range* presents a major *constraint* regarding the robot's kinematics.

3 Engineering Approach and First Prototype

In a first approach the selection of the parallel structure was limited to one variant: Each kinematic leg chain consists of a vertically aligned linear drive and two passive universal joints, representing the common *linear Delta robot* [3, 8], see Fig. 2, left. Since both the inner and outer axes of the two universal joints are parallel to each other, a change in orientation is prevented, cf. [2–5], see Fig. 2, middle.

The system only has three translational degrees of freedom, required for handling the sample tubes during cryopreservation. In preceding works, a MATLAB tool was developed for a dimensional synthesis of this specific structure in the confined space. The main goal was to determine the parameter set from the set of possible combinations of the geometric

parameters, in which the required joint angle ranges of the passive, solid-state joints are minimal. In addition, the optimal installation angles of the passive joints were calculated, at which the deflections from the rest position are minimal. Also, a workspace analysis was carried out for the determined optimum parameter set. A comprehensive description of the developed MATLAB tool based on a particle swarm optimization is omitted for the sake of brevity. The analysis showed that the optimized structure with a maximum angle range of the passive joints of only 46° experiences the least stress in the passive joints but poses the danger of singularities of the first type. Singularities of this type lie on the boundaries of the workspace and result, for example, from the stretching positions of individual link chains. It was assumed, that presetting the inclination in the universal joints to 26° would make it possible to avoid any singularities of the first type. Furthermore it was anticipated, that a larger inclination would reduce the necessary drive forces and thus result in smaller and more cost-effective drives. Due to the nature of the kinematic chains, the working space of the developed parallel robot structure can be represented as an overlap of three cylinders, in the sectional area of which the square area to be covered is located, which contains the bearing racks and the scanner. The minimum achievable application range of the actuator platform is, therefore a circle with the radius 141.42 mm. Based on the workspace restrictions in Sect. 2.1, the resulting bar length was calculated to 334.6 mm. As an illustration, a possible configuration of the resulting parallel robot is shown in Fig. 2. However, the construction shown here is only one of many possible configurations. With the experience gained from the reasoning of the manual design phase, the following systematic synthesis is performed in order to explore all possible solutions for the task and validate the preliminary design.

4 Combined Structural and Dimensional Synthesis

The parallel handling robot can – theoretically – be built up of a vast amount of possible leg chains [4, 5]. With a *structural synthesis* similar to [5], 51 unique leg chains consisting of revolute (R), prismatic (P) and universal (U) joints were identified for the cryogenic handling task described above. In the following, only serial kinematic leg chains without the parallelogram elements of Fig. 2 are selected. In a possible design step after the synthesis, joints with parallel axes can be kinematically replaced by parallelograms [3]. The alignment of base and platform coupling joint is not considered explicitly in textbooks on structural synthesis [4, 5]. However, to make use of the structural synthesis in combination with the dimensional synthesis, this aspect plays a crucial part. A general set of four possible alignments of the base coupling joint (radial, tangential, vertical or conically inclined to the base circle) and three alignments of the platform coupling joint (vertical, tangential and radial to the platform circle) are selected for evaluation. A brute-force approach by performing the dimensional synthesis for all $51 \times 4 \times 3$ combinations without task constraints has proven to be feasible, allowing automation and avoiding symbolic calculations, e.g. of screw vectors

[4]. Not all combinations provide a feasible parallel robot with full mobility and only 328 remaining valid structures are stored in a database. As minimizing motion in the area of thermal insulation is a hard requirement, only the vertical and conically inclined alignment of actuated prismatic base coupling joints is taken into consideration.

This leaves 33 specifiable parallel robots for the following *dimensional synthesis*, where the kinematic parameters of these structures are optimized. The 5–10 optimization parameters (depending on the structure) include the base and platform size and the inclination of conical base joints. Kinematic lengths are expressed with the Denavid-Hartenberg (DH) parameters in the notation of Khalil. An additional offset length between the prismatic joint and the next revolute joint is added to separate joints in cold and warm areas.

The robot is modeled to be of an aluminum alloy with thin struts as hollow cylinders (⌀53 mm, strength 3 mm) and a thin circular platform plate (strength 10 mm). An additional payload of 3 kg at the platform takes the gripper into account. The robot structure is modeled with rigid body dynamics by neglecting link elasticity [16]. The flexure hinges, i.e. all passive joints, are assumed to have a linear joint elasticity. The stiffness of 1.4 N m/27.5° is obtained using the finite element method within ANSYS of the joint depicted in Fig. 2, [15]. A reference trajectory for a pick-and-place application between the two racks as described in Sect. 2 is simulated for 37 positions. The inertial forces are simulated, but only play a minor part compared to forces from gravity and joint elasticities.

The *overall procedure of the dimensional synthesis* of a single robot structure was extended w.r.t. the authors previous work [16] and is sketched in Fig. 3. The *first major step* of the fitness function for a particle is the calculation of the inverse kinematics (IK) in all

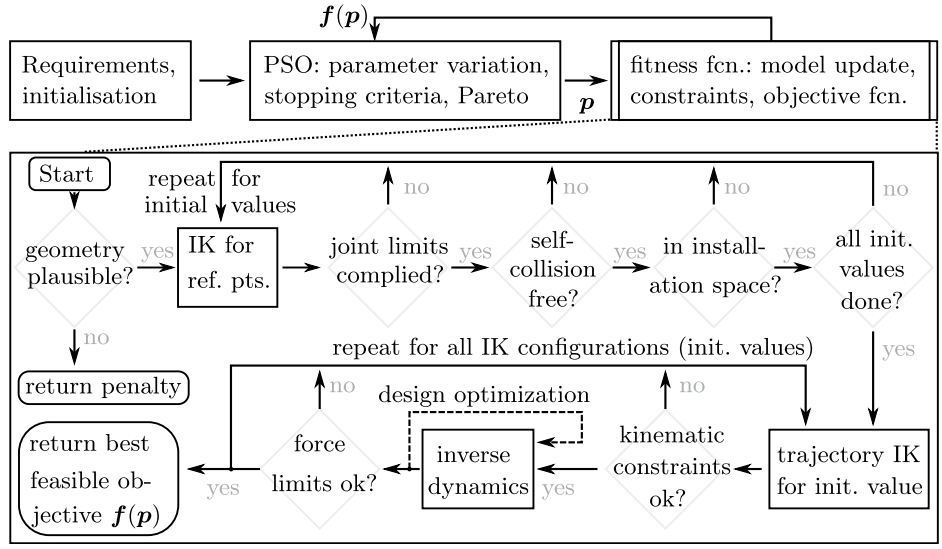

Abb. 3 Overall procedure for the dimensional synthesis of a robot

configurations for the 37 reference points. The IK configurations ("elbow up/down") are found by setting random initial values for the gradient-based IK algorithm and significantly change the outcome of the fitness evaluation, as constraints in this task are mostly only complied in one configuration. The violation of a constraint immediately leads to the abortion of the current configuration with the corresponding penalty term. After the computation of the IK, the prismatic joint offset is determined using a trust-region optimization and geometric considerations. This slightly influences the inertial forces due to the offset's mass. As a *second step*, the trajectory inverse kinematics and dynamics is calculated for all valid configurations, using a general methodology [2, 5, 16]. All constraints are again checked for the trajectory.

As the torques of the joint elasticities (considered as torsion springs) and therefore the actuator forces strongly depend on the flexure hinge rest positions, these present additional design parameters. A choice of the rest positions in the middle of the joint range for the trajectory minimizes the spring torque, but not the actuator forces, which present the design objective.

Therefore, an additional *design optimization* is performed for the rest positions of the flexure hinges as four parameters, assuming a symmetric robot. A pretensioning of the flexure hinges within the 55° angle range was allowed, producing a partial compensation of gravity by the spring torque. The design optimization loop is performed using a single-objective PSO minimizing the maximal actuator force.

The *constraints* are checked in the order of graveness of their violation and the computational effort to determine them. This presents a variation of the PSO "static penalty" approach [11] (static w.r.t. iteration count), termed "hierarchical constraints" in this work [16]. Examples of checked constraints in this order are

- geometric plausibility (leg length matching base/platform),
- success of the inverse kinematics (using a gradient-based solution),
- range of joint angles ($< 55°$ for the flexure hinges),
- self-collisions (using capsules as elementary geometry and axis-aligned bounding boxes as a first check),
- installation space (joint positions have to be inside the cylinder of Fig. 1),
- everything aforementioned for the trajectory IK,
- condition number of the manipulator Jacobian (< 200),
- actuator force in a reasonable range ($< 100\,\mathrm{N}$),
- material stress (within a 50% safety distance of the material's limits).

The violation of an earlier check leads to a higher *penalty term* for the fitness value, where each constraint has a reserved range of values and all constraints are continuous depending on the degree of their violation (corresponding to inequality constraints). Each constraint violation leads to an immediate abortion of the current iteration to reduce the computational effort.

By this means, the time for one fitness evaluation ranges from nearly 0 s (quick check for invalid geometry or failure in reference point IK) over 0.5 s (kinematics constraints after trajectory IK), to 1.8 s (full objective function without additional design optimization) and 13 s (including design optimization of spring rest positions with 120 evaluations of the inverse dynamics). The computation was performed on a state-of-the-art Intel Xeon computing cluster system, using a MATLAB implementation. If all constraints are met, the maximum position error and the maximum actuator force are taken as two *objective functions*, using the multi-objective PSO algorithm from [10]. The position error is obtained by standard methods from [2] (with absolute values of the manipulator Jacobian), assuming 10 µm encoder accuracy of the linear drives. The physical values are normalized and saturated to a value smaller than the constraint penalties [16].

If a constraint is violated, both fitness values are equally set to the penalty. The feasible results and good convergence of the optimization show that the advantages of this approach (no constraint handling parameters, computationally efficient, MATLAB implementation available [10]) prevail the disadvantages (loss of diversity in the particle swarm [11]) for the optimization problem at hand.

5 Discussion of the Results of the Synthesis

Using the presented framework with 9 repetitions of the dimensional synthesis, 100 generations and 100 particles each, results with qualitatively good convergence were obtained for robots 5–12 displayed in Figs. 4 and 6, with around 500 valid results out of the 10,000 evaluations of the fitness function. Every optimization in this setting only takes about one to three hours (on the computing cluster), depending on the success rate and the IK convergence rate. Robots 1–4 of Fig. 4 needed more evaluations, which were provided by running 50 generations with 400 particles and an initial population consisting of the best results of the previous runs. The causing complexity of the kinematics can be deduced from the figures and the number of parameters n, ranging from 5 to 10. The Pareto fronts of all repetitions are combined into one and are shown in Fig. 5. A position accuracy of 40 µm was selected as a reference for the following detailed comparison in Table 1. Of the 33 different structures discussed above, 18 remain which fulfill the constraints and are regrouped for the sake of simplification (by neglecting their difference in platform coupling) to 12 remaining robots.

The structures 1–4 are clearly dominant over all others due to their actuation force lower than 40 N. However, the kinematic structure of numbers 3 and 4, visible in Fig. 4, is significantly more complicated than the engineering solution (structure 9 in Fig. 6), making their realization less likely. Structures 1 and 2 have moderate complexity and are even able to reach full isotropy ($\mathrm{cond}(\boldsymbol{J}) = 1$ in the whole workspace) for some particles on the Pareto front, which generally is very favorable [5]. A detailed analysis shows that a low actuator force in general is mainly enabled by a compensation of the effects of gravity and joint

elasticity, together with a good force transmission from actuators to platform. From other runs of the optimization it is known that passive joint angle ranges of only 22° are possible for some structures, but the optimal results are over 40°. Therefore minimizing the angle range or the elastic joint torque does not directly benefit this objective, supporting the results from Sect. 3.

The 3PRUR-structures (numbers 5 and 6) present the second best alternative, as an actuator force of 56 N can be achieved with a conical alignment of the prismatic joints. The engineering solution of Sect. 3 corresponds to the 3PUU-kinematics (number 9), which has a similar performance as structures number 7 to 12. The engineering solution is evaluated in the last row of the table and also lies on the Pareto front, validating the different tools. All these structures (number 7 to 12) have a similar parallel and vertical alignment of joint axes, noted by ȒŔŔȒ. The main difference between numbers 7/8, 9/10 and 11/12 is the replacement of ȒŔ-pairs of revolute joints by universal joints, which sets the intermediate DH parameters to zero, but does not change the kinematic structure. For these structures a conical joint alignment is not sufficiently beneficial.

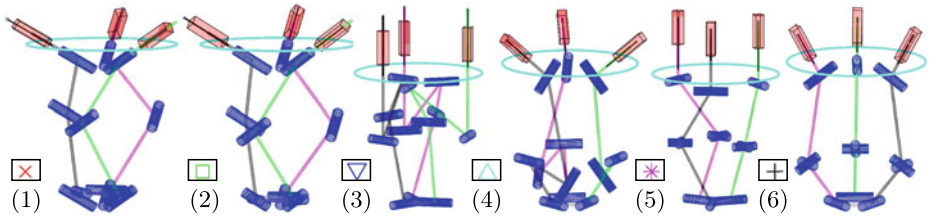

Abb. 4 Visualization of selected robot kinematics from Table 1 with markers from Fig. 5. Leg chains are printed in different colors and the circle marks the tank's upper edge

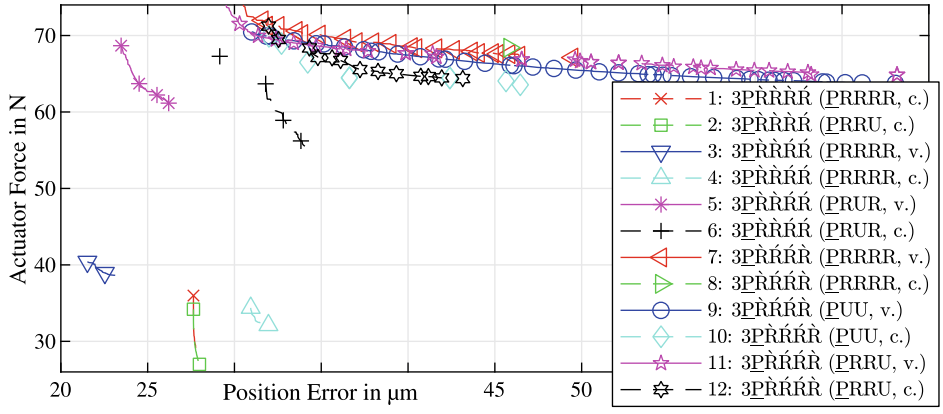

Abb. 5 Pareto fronts for all robot structures. The parallel robot notation is taken from [2] and the kinematic chain notation is taken from [4], where all Ȓ and Ŕ are parallel to each other, respectively. Base alignment noted with "v" (vertical) and "c" (conical)

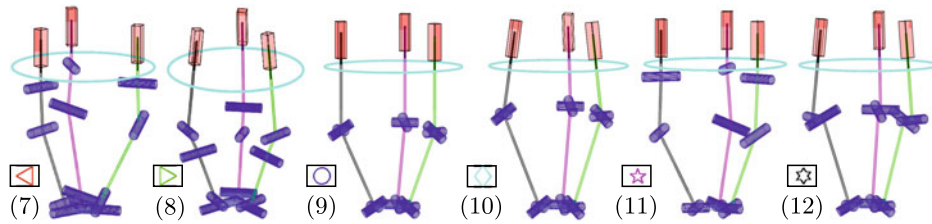

Abb. 6 Second half of the robot kinematics visualizations from Table 1

Tab. 1 Summary of one typical particle for each robot from the Pareto front. Abbreviations: "Cond." (condition number of Jacobian), range (of passive joint angles), mass (articulated, legs and platform without payload), n (number of optimization variables), r_B (base radius), φ_B (prismatic joint inclination), r_P (platform radius), q_{1off} (prismatic joint offset), a_i,d_i (DH parameters). Row "Eng.": engineering solution from Fig. 2

		Performance					Kinematic parameters									
		Err. µm	Force N	Cond.	Range deg	Mass kg	n	r_B mm	φ_B mm	r_P deg	q_{1off} mm	a_3 mm	d_3 mm	a_4 mm	d_4 mm	a_5 mm
1	×	28	28	1.2	51.0	4.3	10	374	59	81	208	263	135	332	144	24
2	□	28	27	1.1	49.3	4.2	9	359	57	83	200	271	164	309	127	—
3	▽	23	39	5.3	53.7	6.1	8	223	0	80	408	330	106	151	91	390
4	△	32	32	3.5	46.8	5.1	9	297	50	80	212	314	316	151	118	233
5	✳	26	61	2.5	46.7	4.2	6	206	0	80	235	282	150	—	—	307
6	+	34	56	2.5	53.0	3.7	7	252	30	80	164	275	229	—	—	222
7	◁	40	69	3.8	40.8	3.6	8	225	0	80	158	165	52	321	143	34
8	▷	44	81	3.8	40.3	3.8	9	177	174	81	367	109	28	258	47	20
9	○	40	67	3.4	36.9	3.6	5	225	0	80	369	—	—	347	41	—
10	♢	42	64	3.9	33.5	3.6	6	191	172	80	306	—	—	399	104	—
11	☆	40	68	3.8	40.5	3.6	7	225	0	80	153	204	97	323	94	—
12	✡	40	65	3.5	34.4	3.7	8	207	174	80	327	22	38	374	69	—
Eng.		37	67	3.1	39.3	3.6	6	230	0	80	395	—	—	335	0	—

6 Summary and Outlook

Enhancing the assumptions in the combined structural and dimensional robot synthesis with knowledge from the engineering approach allows to vastly reduce the complexity of the optimization problem, without limiting the combined synthesis in the highly constrained cryogenic handling task. The comparison already proves the feasibility of the chosen design relative to other possible structures. The theoretical improvement of a design change is quantified to reduce the already low actuator force about 60%. This would require using two single revolute joints instead of one universal joint and may reduce the structural stiffness. Further investigations on replacing consecutive parallel joints by parallelogram subchains

have to be performed before considering the design change. The findings on compensating gravity with elastic joint moments may be used in a pretensioning of the flexure hinges and in the control of the robot.

Danksagung The authors acknowledge the support by the Deutsche Forschungsgemeinschaft (DFG) under project numbers 341489206 (combined synthesis) and 349906175 (cryogenic handling). MATLAB code to reproduce the results is available at GitHub under https://github.com/SchapplM/robsynth-paper_mhi2021.

Literatur

1. Borchert, G., Löchte, C., Brumme, S., Carbone, G., Ceccarelli, M., Raatz, A.: Design methodology for a compliant binary actuated parallel mechanism with flexure hinges. In: F. Viadero, M. Ceccarelli (eds.) New Trends in Mechanism and Machine Science, pp. 171–179. Springer, Netherlands, Dordrecht (2013). https://doi.org/10.1007/978-94-007-4902-3_18
2. Merlet, J.P.: Parallel robots. Solid Mechanics and Its Applications, vol. 128, 2nd edn. Springer Science & Business Media (2006). https://doi.org/10.1007/1-4020-4133-0
3. Frindt, M., Krefft, M., Hesselbach, J.: Structure and type synthesis of parallel manipulators. In: Robotic Systems for Handling and Assembly, pp. 17–37. Springer (2010). https://doi.org/10.1007/978-3-642-16785-0_2
4. Kong, X., Gosselin, C.M.: Type Synthesis of Parallel Mechanisms. Springer, Berlin (2007). https://doi.org/10.1007/978-3-540-71990-8
5. Gogu, G.: Structural synthesis of parallel robots, part 1: methodology. Solid Mechanics and Its Applications, vol. 866. Springer, Netherlands (2008). https://doi.org/10.1007/978-1-4020-5710-6
6. Krefft, M.: Aufgabenangepasste Optimierung von Parallelstrukturen für Maschinen in der Produktionstechnik. PhD thesis, Technische Universität Braunschweig (2006)
7. Stock, M., Miller, K.: Optimal kinematic design of spatial parallel manipulators: application to linear delta robot. J. Mech. Des. **125**(2), 292–301 (2003). https://doi.org/10.1115/1.1563632
8. Kelaiaia, R., Company, O., Zaatri, A.: Multiobjective optimization of a linear delta parallel robot. Mech. Mach. Theory **50**, 159–178 (2012). https://doi.org/10.1016/j.mechmachtheory.2011.11.004
9. Jamwal, P.K., Hussain, S., Xie, S.Q.: Three-stage design analysis and multicriteria optimization of a parallel ankle rehabilitation robot using genetic algorithm. IEEE Trans. Autom. Sci. Eng. **12**(4), 1433–1446 (2015). https://doi.org/10.1109/TASE.2014.2331241
10. Coello, C.A.C., Pulido, G.T., Lechuga, M.S.: Handling multiple objectives with particle swarm optimization. IEEE Trans. Evol. Comput. **8**(3), 256–279 (2004). https://doi.org/10.1109/TEVC.2004.826067. Code from V. Martínez-Cagigal
11. Mezura-Montes, E., Coello, C.A.C.: Constraint-handling in nature-inspired numerical optimization: past, present and future. Swarm Evol. Comput. **1**(4), 173–194 (2011). https://doi.org/10.1016/j.swevo.2011.10.001
12. Hesselbach, J., Raatz, A., Kunzmann, H.: Performance of pseudo-elastic flexure hinges in parallel robots for micro-assembly tasks. CIRP Ann. **53**(1), 329–332 (2004). https://doi.org/10.1016/S0007-8506(07)60709-4

13. Fowler, R., Maselli, A., Pluimers, P., Magleby, S., Howell, L.L.: Flex-16: a large-displacement monolithic compliant rotational hinge. Mech. Mach. Theory **82**, 203–217 (2014). https://doi.org/10.1016/j.mechmachtheory.2014.08.008
14. Henein, S., Spanoudakis, P., Droz, S., Myklebust, L.I., Onillon, E.: Flexure pivot for aerospace mechanisms. In: 10th European Space Mechanisms and Tribology Symposium, San Sebastian, Spain, pp. 285–288 (2003)
15. Jahn, P., Raatz, A.: Numerical simulation and statistical analysis of a cascaded flexure hinge for use in a cryogenic working environment. In: Annals of Scientific Society for Assembly, Handling and Industrial Robotics, pp. 81–94. Springer, Berlin (2020). https://doi.org/10.1007/978-3-662-61755-7_8
16. Schappler, M., Ortmaier, T.: Dimensional synthesis of parallel robots: unified kinematics and dynamics using full kinematic constraints. In: 6. IFToMM D-A-CH Konferenz. Lienz, Österreich (2020). https://doi.org/10.17185/duepublico/71211